PLASMA CONFINEMENT STUDIES IN LHD

M.FUJIWARA, H.YAMADA, A.EJIRI, M.EMOTO, H.FUNABA, M.GOTO, K.IDA, H.IDEI, S.INAGAKI, S.KADO, O.KANEKO, K.KAWAHATA, A.KOMORI, S.KUBO, R.KUMAZAWA, S.MASUZAKI, T.MINAMI, J.MIYAZAWA, T.MORISAKI, S.MORITA, S.MURAKAMI, S.MUTO, T.MUTOH, Y.NAGAYAMA, Y.NAKAMURA, H.NAKANISHI, K.NARIHARA, K.NISHIMURA, N.NODA, T.KOBUCHI, S.OHDACHI, N.OHYABU, Y.OKA, M.OSAKABE, T.OZAKI, B.J.PETERSON, A.SAGARA, S.SAKAKIBARA, R.SAKAMOTO, H.SASAO, M.SASAO, K.SATO, M.SATO, T.SEKI, T.SHIMOZUMA, M.SHOJI, H.SUZUKI, Y.TAKEIRI, K.TANAKA, K.TOI, T.TOKUZAWA, K.TSUMORI, K.TSUZUKI, I.YAMADA, S.YAMAGUCHI, M.YOKOYAMA, K.Y.WATANABE, T.WATARI, R.AKIYAMA, H.CHIKARAISHI, K.HABA, S.HAMAGUCHI, M.IIMA, S.IMAGAWA, N.INOUE, K.IWAMOTO, S.KITAGAWA, Y.KUBOTA, J.KODAIRA, R.MAEKAWA, T.MITO, T.NAGASAKA, A.NISHIMURA, Y.TAKITA, C.TAKAHASHI, K.TAKAHATA, K.YAMAUCHI, H.TAMURA, T.TSUZUKI, S.YAMADA, N.YANAGI, H.YONEZU, Y.HAMADA, K.MATSUOKA, K.MURAI, K.OHKUBO, I.OHTAKE, M.OKAMOTO, S.SATOH, T.SATOW, S.SUDO, S.TANAHASHI, K.YAMAZAKI, O.MOTOJIMA, A.IIYOSHI
National Institute for Fusion Science,
Toki, Gifu,
Japan

Abstract

The initial experiments of the Large Helical Device (LHD) have extended confinement studies on currentless plasmas to a large scale (R=3.9 m, a = 0.6 m). Heating by NBI of 3 MW has produced plasmas with a fusion triple product of 8×10^{18} keVm^{-3}s at a magnetic field of 1.5T. An electron temperature of 1.5 keV and an ion temperature of 1.1 keV have been achieved simultaneously at the line-averaged electron density of 1.5×10^{19} m^{-3}. The maximum stored energy has reached 0.22 MJ with neither unexpected confinement deterioration nor visible MHD instabilities, which corresponds to $\langle\beta\rangle$ =0.7%. Energy confinement times, reaching 0.17 s at the maximum, have shown a similar manner to the present scaling law derived from the existing medium sized helical devices, but improve on it by 50%. A distinguishing feature of a favorable dependence of energy confinement time on density remains in the present power density (~40kW/m^3) and the electron density (3×10^{19}m^{-3}) regimes unlike L-mode in tokamaks. High edge temperatures of both electrons and ions as high as 200 eV have been observed at the outermost flux surface, which indicate a qualitative jump in performance from the helical devices to date. Spontaneously generated toroidal currents agree with the physical picture of neoclassical bootstrap currents. Change of magnetic configuration due to finite-β effect has been well described by the 3-D MHD equilibrium analysis. An escape of particles from the core region leading to a hollow density profile has been observed in hydrogen plasmas, which is mitigated through core fueling with a pellet injection or in helium discharges.

1. INTRODUCTION

The physics research goal of the Large Helical Device (LHD) [1,2] is to achieve and study currentless plasmas which can be extrapolated to the reactor condition in a heliotron configuration. The minor radius of 0.6 m is prerequisite to separate the core region confining high temperature plasmas from the boundary where atomic processes play an essential role. This paper describes the first experiments with regard to confinement studies under conditions that the helical devices had not satisfied to date. LHD has the major radius of 3.9 m and the operated magnetic field in this study is 1.5 T although superconducting coils have capability of 3 T operation [3]. Progress in experiments

of helical devices (CHS, Heliotron E, Wendelstein VII-AS, and ATF) in the last decade [4] has demonstrated performance equivalent to L-mode plasmas in tokamaks with similar dimensions and has indicated clear clues for further confinement improvement [5-7]. The first primary subject in this study lies in the clarification of the extrapolation of prior experience to large-scale plasmas which are sufficiently collisionless.

The magnetic geometry in this study is set at the optimized one from MHD stability, neoclassical transport and particle confinement. The magnetic axis is 3.75 m which is inward shifted from the machine center and the averaged elongation is 1. The plasma vacuum vessel which also functions as the first wall is stainless steel and is conditioned by discharge cleanings of He glow or ECR (2.45GHz) DC plasmas, and by Ti gettering with a coverage area of 20 %. The 2nd harmonic 84-GHz ECH up to 400 kW has been employed to generate plasmas, which are targets for NBI. The ray of ECH is well focused with waist sizes of 50 mm in the toroidal direction and 15 mm in the radial direction. Since the focal point is controllable by movable mirrors, the deposition profile effect on transport and kinetic effect of power deposition with relation to the magnetic geometry can be examined. Two negative-ion-based neutral beam injectors are aligned for tangential injection in opposing directions relative to the helical coil current (co- and counter-injections) to operate plasmas free from beam driven toroidal currents. Each injector is designed to inject a 7.5 MW hydrogen beams at an energy of 180keV for 10 s. One of the injectors is also designed to inject 100 keV beams of 0.5 MW up to 90 s. In the initial experiments, the ion sources are optimized for a lower energy up to 100 keV considering that the target plasma density is low under the 1.5 T operation. In this study the available injecting beam power is 3 MW in total. Profile measurements are available by YAG-laser Thomson scattering for the electron temperature, charge-exchange-recombination spectroscopy (CXRS) for the ion temperature and multi-chord FIR interferometer for the electron density.

2. CHARACTERISTICS OF PLASMA DISCHARGE

ECH produces target plasmas with a density of more than 1×10^{19} m^{-3} so as to have the shine-through power of NBI less than 40%. Waveforms of a typical hydrogen discharge are shown in Fig.1(a). The plasma expands in the radial direction with increasing temperature and density during the initial 0.5 s. When the high-temperature plasma reaches the magnetic boundary, a divertor channel is formed. The events of a rapid pump-out of density, a decrease of radiation and bursts of divertor flux start with regard to this timing. The decay time of the decrease in density is enhanced by an increase of the heating power. Density does not build up efficiently despite strong gas puffing in the pump-out phase for several hundreds ms. A pellet injection is effective in increasing density as well as the stored energy, however, the decay constant of the density is not improved. Typical electron density, temperature and particle flux on the divertor plates in this phase are 5×10^{17} m^{-3}, 10 to 20 eV and 10^{22} m^{-2}/s, respectively. The amplitude of the oscillation in the particle flux is about 50% and no obvious peaks in the power spectrum have been observed. In the discharges which are longer than 1 s, density clamping is terminated in the later phase. Since the stainless steel becomes occluded at around 1×10^{22} hydrogenic ions per m^2, this phenomena can be explained by degradation of pumping efficiency. The pump-out phenomena is much milder and density can be maintained by recycling instead of auxiliary gas puffing in helium discharges since the metallic wall does not pump helium (see Fig.1 (b)). Helium plasmas also mitigate the shine-through losses of NBI in the low density regime.

The present operational density limits bounded by radiation collapses are 4.5×10^{19} m^{-3} in hydrogen plasmas with a gas puff, 6.0×10^{19} m^{-3} in hydrogen plasmas with a pellet injection, and 6.3×10^{19} m^{-3} for helium plasmas. The radiation collapse phenomena can be classified into two types. The first type is characterized by a hollow radiation profile that increased symmetrically up until the radiation collapse. In these instances the peak total radiated power is at or below the beam input power. In these discharges the stored energy drops steadily to zero in a time frame of 100 ms or more. The

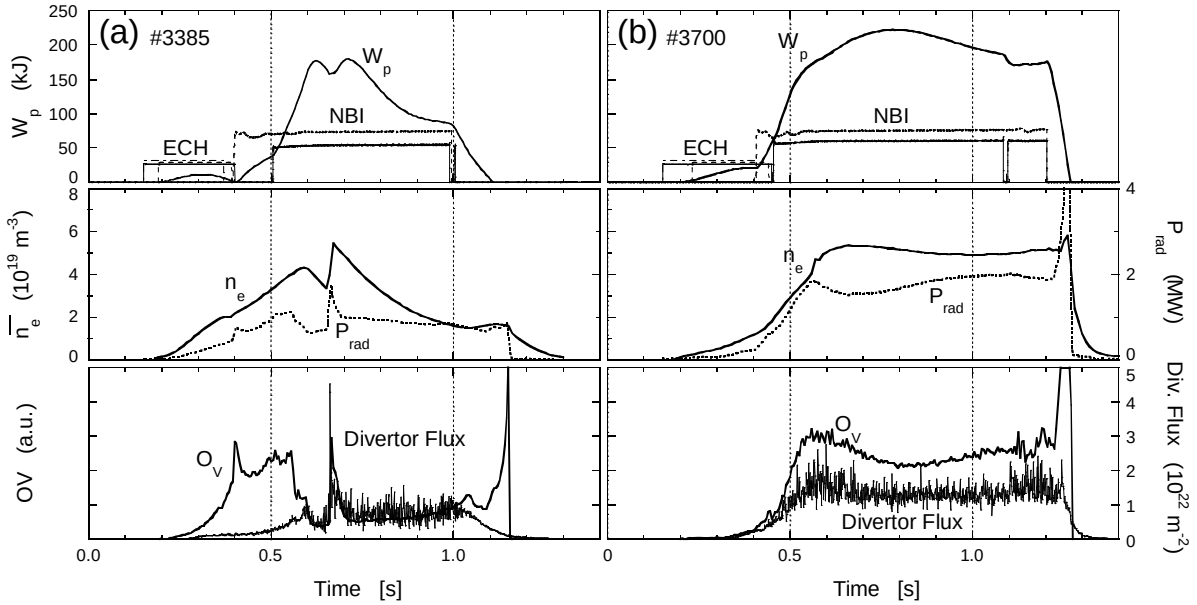

FIG.1. *Typical discharges of NBI heated plasmas. (a) Hydrogen. The pellet is injected at t = 0.81s. (b) Helium.*

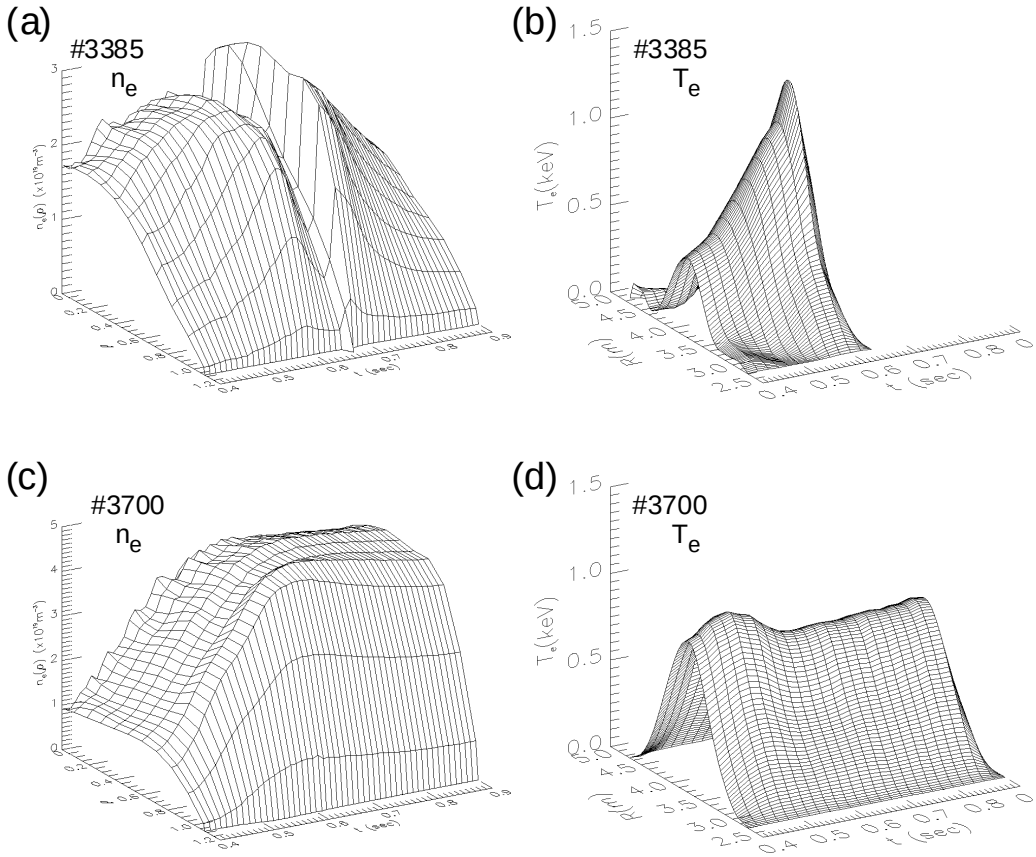

FIG.2. *Evolution of electron density and temperature profiles. Density profiles are derived from Abel inversion from FIR chordal data. Temperatures are measured by the YAG laser (50Hz)-Thomson scattering system. (a) Density profile in a hydrogen discharge. (b) Temperature profile in a hydrogen discharge. (c) Density in a helium discharge. (d) Temperature in a helium discharge.*

second type is characterized by a rapid increase in the total radiated power over a 100 ms time frame resulting in an instantaneous peak total radiated power, which is well in excess of the input heating power. The detector profile shows a sharp peaking on the inboard side of the plasma which increases and moves towards the center of the plasma in 30 ms.

Figure 2 illustrates the evolution of density and temperature profiles in the discharges shown in Fig.1. In a hydrogen discharge, a broad density profile becomes hollow when the pump-out starts. Pellet injection (3 mm in diameter and 3 mm in length, particle inventory of 10^{21}) has mitigated the hollow density profile. Broad density profile is maintained throughout a helium discharge and the edge density is higher than that in a hydrogen discharge, which is due to a larger neutral source from recycling. The temperature profile is more peaked in a hydrogen discharge than a helium one.

While hydrogen discharges are accompanied by the density pump-out, the low recycling condition which has been strongly related to confinement improvements has been realized. The temperatures of both electrons and ions have reached 200 eV at the outermost flux surface and the density is sharply bounded at the outside of the last closed flux surface (see Fig.3). Although a clear significant improvement of confinement has not been observed yet, the above mentioned density and temperature characteristics have not been observed in the helical devices to date and the increase of

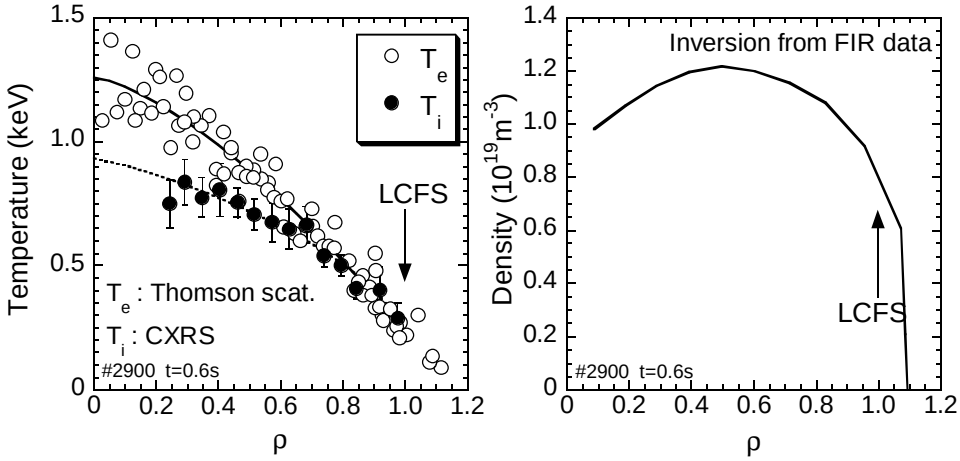

FIG.3. *Typical radial profiles of ion and electron temperatures and electron density in the pump-out low-recycling phase*

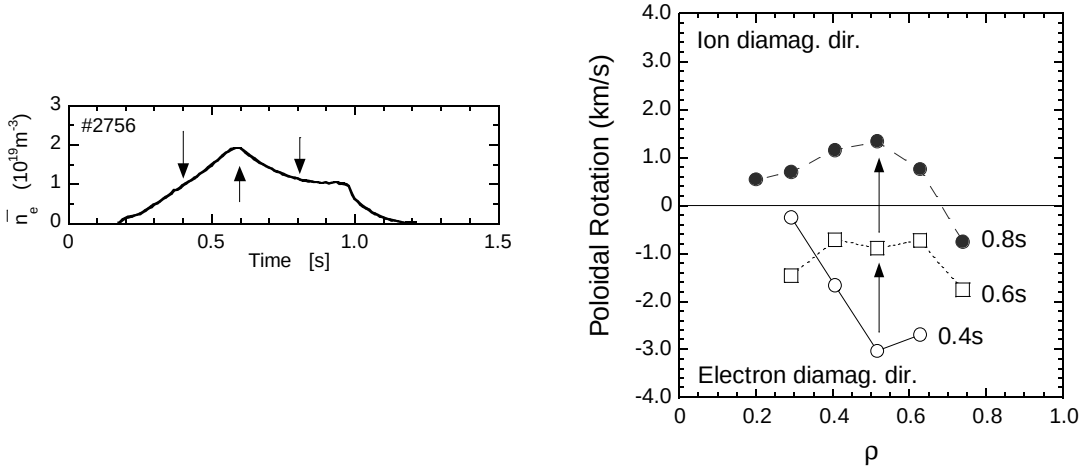

FIG.4. *Change of poloidal rotation before (t = 0.4s), at (t=0.6s) and during (t=0.8s) the event of the density clamping.*

edge temperatures which is a key of confinement improvement would be expected by increased input power in further experiments.

The poloidal rotation which is closely connected to the radial electric field E_r has been measured by CXRS. A change in the direction of the rotation has been observed before and after the start of pump-out in a hydrogen discharge. Figure 4 indicates that the plasma rotates initially in the electron diamagnetic direction and then changes to the ion diamagnetic direction. This may reflect a change in the sign of E_r from negative to positive. Hollow density profiles are enhanced by the positive electric field [8] and a neoclassical theory has pointed out that this problem is pronounced in large-scale plasmas [9].

3. GLOBAL CONFINEMENT

Four major inter-machine scalings of energy confinement time for helical devices (LHD scaling [10], Lackner-Gottardi scaling [11], gyro-reduced Bohm [12] and International Stellarator Scaling 95 (ISS95) [13]) have been proposed so far and all describe similar manners of power deterioration and positive density dependences. The international stellarator scaling 95 (ISS95) expresses,

$$t_E = 0.079 a^{2.21} R^{0.65} P^{-0.59} \bar{n}_e^{0.51} B^{0.83} \iota_{2/3}^{0.4}$$

where τ_E in s, a and R in m, P in MW, $\bar{n}_e$ in 10^{19}m^{-3}, and B in T. While this scaling describes L-mode plasmas in large tokamaks as well, density dependence is pronounced unlike in the tokamak L-mode scaling. From experience in tokamaks, larger devices which have less heating power density make the transition to saturation from linear ohmic confinement in the lower density regime, which is connected to an L-mode with auxiliary heating. This issue is crucial for the prospects of helical devices since the present reactor design relies on the favorable density dependence on confinement.

Energy confinement times are estimated by the stored energy measured by diamagnetic loops. The response of diagmagnetic loops has been calculated by the 3-D magnetic field analysis with 3-D finite-β equilibria. The NBI power deposition is modeled by the database from a number of runs of a

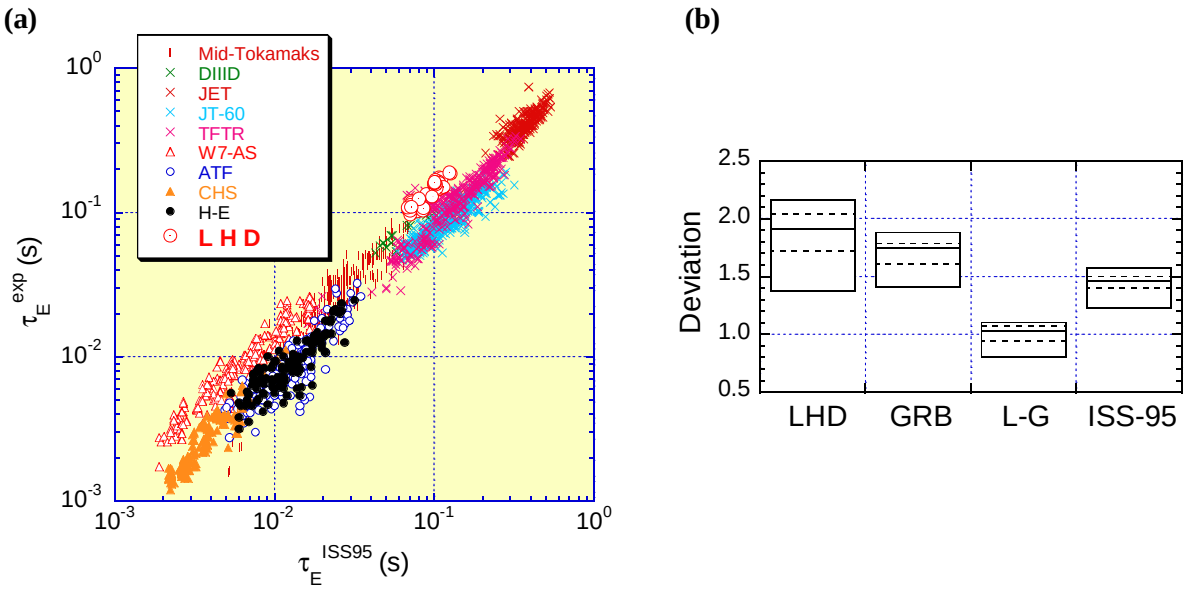

FIG.5. *(a) Comparison of experimental energy confinement times with those predicted by ISS95. Data from helical device are adapted from the international stellarator database and data from tokamaks are adapted from the ITER L-mode database (S.M.Kaye et al., Nucl. Fusion **37** (1997) 1303) (b) Deviation of experimental data from the scalings. LHD: the LHD scaling, L-G: the Lackner-Gottardi scaling, GRB: the gyro-reduced Bohm scaling and ISS95: the international stellarator scaling .*

3-D Monte-Carlo simulation code, MCNBI [14]. In heliotrons a large Shafranov shift occurs at finite β to change the beam birth profile and the drift orbit of beam particles. Therefore, in the code, the 3-D magnetic configuration including the finite-β effect is used for the evaluation of the deposition profile. The computational results suggest that heating efficiency and deposition profiles are not different for the cases of co- and counter- injections in the current experimental condition. The stored energy derived from kinetic measurements agrees with the diamagnetic measurement, which is consistent with the fact that results from the NBI power deposition model suggest a negligible effect from the beam pressure (at most a few %).

Figure 5 (a) shows the comparison of experimental data with the prediction from the ISS95 expression. The density and power absorption ranges cover $1.0 - 5.0\times10^{19}$ m^{-3} and 0.5 – 2.3 MW. The data in hydrogen discharges have been adopted here, since the estimate of power deposition in helium discharges cannot be discussed with the same accuracy as in hydrogen now. While the trend of energy confinement times of NBI heated plasmas in LHD has a manner similar to ISS95, experimental data is systematically better than ISS95 by a factor of 1.5. Deviation from the scalings indicates an enhancement of a factor of 2 from the LHD scaling and is comparable to the L-G scaling (see Fig. 5 (b)).

High density plasmas with a pellet injection and one NBI have almost the same absorption power as low density ones with two NBI's. Comparison of those sequences indicates that energy confinement is improved with the square root of the density in the accessible the density range (3×10^{19} m^{-3}) with a power density of 40 kW/m^3.

4. MHD CHARACTERISTICS

The MHD equilibrium properties have been well described by 3-D finite-β equilibrium calculation in helical devices [15]. Since the volume averaged beta <β> has reached 0.7%, The theory predicts the Shafranov shift of 14 cm on the prolate cross-section and 23 cm on the oblate one. Figure 6 shows the shift of the peak of the soft X-ray profile which corresponds to the magnetic axis. Since the increase of β is primarily attributed to the increase in density, the pressure profile is flattened in the higher β region in accordance with broadening of the density profile. The experimental estimates agree with the finite-β calculation very well. Also, a similar change of plasma profiles has been observed in the density and the electron temperature.

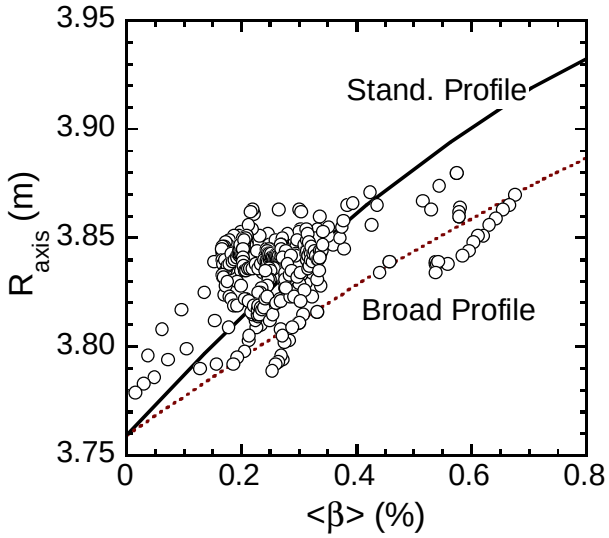

FIG.6. *Shift in peak of the soft-X ray profile. Lines indicate estimates from the 3-D MHD computation. Solid line : assume a standard profile from* $p=p_0(1-r^2)^2$. *Broken line : assume a broad profile from* $p=p_0(1-r^2)(1-r^8)$.

No internal relaxation phenomena have been observed in the core region so far. Spontaneous generation of a magnetic well due to the Shafranov shift realizes Mercier (ideal interchange mode) stable configuration leading to the equilibrium limit.

5. GENERATION OF TOROIDAL CURRENTS

Research in both tokamaks and helical devices [16,17] has confirmed neoclassical bootstrap currents. The magnetic field of LHD is excited in a real steady state with using superconducting coils. Therefore, the applied voltage is extremely low and ohmic currents are absolutely excluded. The capability for long-pulse discharges can also eliminate the ambiguity of time dependent behaviors. A precise investigation will progress in LHD making full use of these advantages. A toroidal current of up to 50 kA has been observed in a discharge with co-injected NBI of 1.5MW while the equivalent currents to generate the rotational transform in the vacuum magnetic field of LHD is 700 kA at 1.5 T. It takes more than 2 s for currents to reach a steady state, which is comparable to the L/R time of the plasma. Figure 7 (a) shows the dependence of the toroidal currents on density. These currents result from the synergetic effect of bootstrap currents and Ohkawa currents. All currents flow in the paramagnetic direction which increase the rotational transform. Since the bootstrap current is expected to flow in the paramagnetic direction, the total currents shift to this side. Observed currents with co-injection decrease in the high density regime which is explained by the degradation of efficiency of the Ohkawa current. The Ohkawa current is cancelled out in the case of balanced injection and bootstrap current is pronounced. Figure 7 (b) indicates that the toroidal current increases in proportion with the stored energy which reflects pressure gradient. A neoclassical estimate [18] bounds the upper limit of the experimental observation, which is explained by a discharge duration which is too short to ramp the full current.

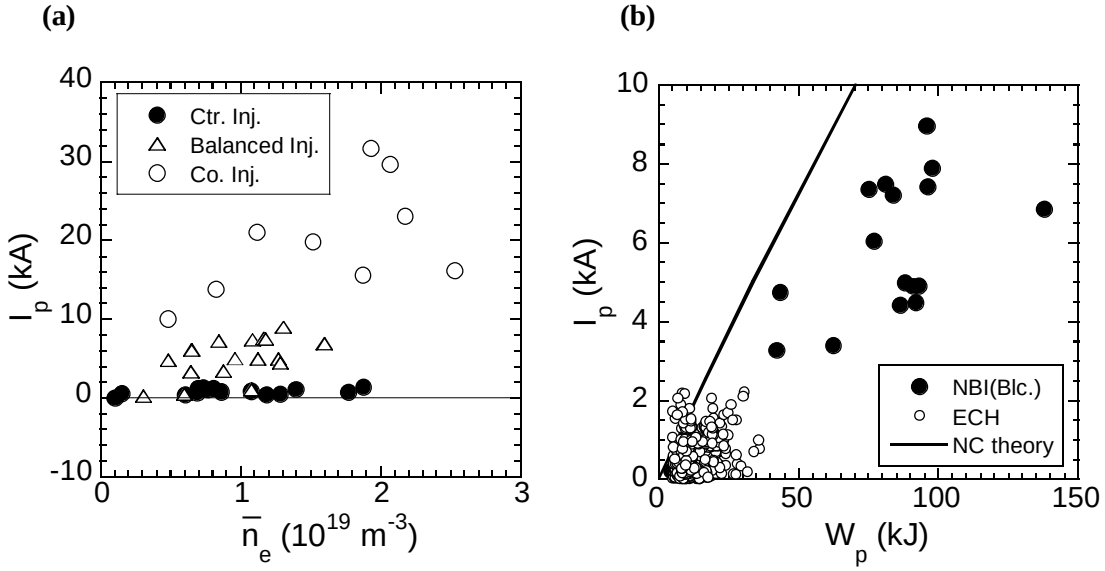

FIG.7. *(a) Toroidal currents as a function of density. (b) Toroidal currents as a function of stored energy. Only the case of balanced injection is illustrated here for NBI. Since the ray of ECH is injected perpendicularly to the magnetic field, no momentum input exists. Lines: prediction from the neoclassical theory by scanning the density profile* $n_e = n_{e0}(1-r^8)$ *with the fixed temperature profile* $T = (1-r^2)$ *(keV).*

6. DISCUSSIONS AND SUMMARY

The initial experiments on the Large Helical Device (LHD) have extended confinement studies on currentless plasmas to a large scale. An outlook of confinement of NBI heated plasmas has shown

a trend similar to the prior scaling laws, however, a significant improvement compared with the ISS95 expression by a factor of 1.5 and comparable data to the Lackner-Gottardi scaling have been obtained. In the present experimental condition, an absorbed power of NBI depends on the operational density. Therefore, it needs a careful attention and further systematic scans to separate the power degradation from a favorable density dependence. Comparison with two kinds of experimental set-up with the same absorbed power, i.e., high density discharges heated by 1 beam with a pellet injection and low density discharges heated by 2 beams is consistent with the prediction that confinement is improved with the square root of density.

Fueling of particle is reconfirmed as an important operational issue in the experiment. An escape of particles from the core of the plasma has been highlighted in hydrogen discharges. Low recycling condition is achieved simultaneously, which leads to high temperatures at the edge. This observation is explained from the concept of the high temperature divertor [19]. Combination with central fueling by pellet injection has mitigated a hollow density profile temporally. Helium discharges facilitates particle control through high recycling. Here it should be noted that the high edge temperature is not specific to hydrogen discharges. A careful control of helium gas puffing can realize a similar high edge temperature.

Heating by NBI of 3 MW has realized plasmas with a fusion triple product of 8×10^{18} keVm^{-3}s at the magnetic field of 1.5T. An electron temperature of 1.5 keV and an ion temperature of 1.1 keV have achieved simultaneously at the line-averaged electron density of 1.5×10^{19} m^{-3}. At the density as low as 4×10^{18}m^{-3}, the central ion temperature reaches 1.4 keV.

Spontaneous generation of toroidal currents has been observed, characteristics of which agree with neoclassical bootstrap currents. Changes of the plasma profile have been well described by the 3-D MHD equilibrium analysis.

ACKNOWLEDGEMENTS

The authors are grateful to all collaboration with universities and institutes. Efforts by the industrial companies to complete the LHD construction are greatly appreciated.

REFERENCES

[1] IIYOSHI, A., et al., these Proceedings.
[2] FUJIWARA, M., et al., J. Fusion Energy **15** (1996)7.
[3] MOTOJIMA, O., et al., these Proceedings.
[4] IIYOSHI, A., in Plasma Physics and Controlled Nuclear Fusion Research 1996 (Proc.16th Conf. Montreal, 1996), Vol.1, IAEA, Vienna (1997) 113.
[5] TOI, K., et al., in Plasma Physics and Controlled Nuclear Fusion Research 1992 (Proc.14th Conf. Würtzburg, 1992), Vol.2, IAEA, Vienna (1993) 461.
[6] ERCKMANN, V., et al., Phys. Rev. Lett. **70** (1993) 2086
[7] IDA, K., et al., Phys. Rev. Lett. **76** (1996) 1268.
[8] IDEI, H., et al., Phys. Plasmas **1** (1994) 3400.
[9] MAASSBERG, H., BEIDLER, C.D., SIMMET, E.E., J.Plasma Fusion Res. SERIES, Vol.1 (1998) 230.
[10] SUDO, S., et al., Nucl. Fusion **30** (1990)11.
[11] LACKNER, K., GOTTARDI, N.A.O., Nucl. Fusion **30** (1990) 767.
[12] MURAKAMI, M., et al., in Plasma Physics and Controlled Nuclear Fusion Research 1992 (Proc.14th Conf. Würtzburg, 1992), Vol.2, IAEA, Vienna (1993) 391.
[13] STROTH, U., et al., Nucl. Fusion **36** (1996) 1063.
[14] MURAKAMI, S., et al., Trans. Fusion Tech. **27** (1995) 256.
[15] YAMADA, H., et al., Nucl. Fusion **32** (1992) 25.
[16] MURAKAMI, M., et al., Phys. Rev. Lett. **66**(1991)707.
[17] YAMADA, H., et al., Nucl. Fusion **34** (1994) 641.
[18] WATANABE, K.Y., et al., Nucl. Fusion **35** (1995) 335.
[19] OHYABU, N., et al., Nucl. Fusion **34** (1994) 387.